THE JOURNAL OF IMMUNOLOGY

Combined Deletion of *Id2* and *Id3* Genes Reveals Multiple Roles for E Proteins in Invariant NKT Cell Development and Expansion

Jia Li, Di Wu, Ning Jiang and Yuan Zhuang

J Immunol 2013; 191:5052-5064; Prepublished online 11 October 2013;
doi: 10.4049/jimmunol.1301252
http://www.jimmunol.org/content/191/10/5052

The Journal of Immunology is published twice each month by
The American Association of Immunologists, Inc.,
9650 Rockville Pike, Bethesda, MD 20814-3994.

Print ISSN: 0022-1767 Online ISSN: 1550-6606.

Combined Deletion of *Id2* and *Id3* Genes Reveals Multiple Roles for E Proteins in Invariant NKT Cell Development and Expansion

Jia Li,* Di Wu,[†,‡] Ning Jiang,[†,‡] and Yuan Zhuang*

The invariant NKT (iNKT) cells represent a unique group of αβ T cells that have been classified based on their exclusive usage of the invariant Vα14Jα18 TCRα-chain and their innate-like effector function. Thus far, the transcriptional programs that control Vα14Jα18 TCRα rearrangements and the population size of iNKT cells are still incompletely defined. E protein transcription factors have been shown to play necessary roles in the development of multiple T cell lineages, including iNKT cells. In this study, we examined E protein functions in T cell development through combined deletion of genes encoding E protein inhibitors *Id2* and *Id3*. Deletion of *Id2* and *Id3* in T cell progenitors resulted in a partial block at the pre-TCR selection checkpoint and a dramatic increase in numbers of iNKT cells. The increase in iNKT cells is accompanied with a biased rearrangement involving Vα14 to Jα18 recombination at the double-positive stage and enhanced proliferation of iNKT cells. We further demonstrate that a 50% reduction of E proteins can cause a dramatic switch from iNKT to innate-like γδ T cell fate in *Id2*- and *Id3*-deficient mice. Collectively, these findings suggest that Id2- and Id3-mediated inhibition of E proteins controls iNKT development by restricting lineage choice and population expansion. *The Journal of Immunology*, 2013, 191: 5052–5064.

Development of T cells in the thymus generates multiple types of T cells that belong to different lineages, defined primarily by the types of TCRs they use. The αβ T lineage is specified after expression of the pre-TCR composed of the TCRβ-chain and the invariant pre–TCRα-chain. These precursor T cells then undergo proliferative expansion before rearranging the TCRα-chain. Upon generation of the αβ TCR, most αβ T cells differentiate into CD8 cytolytic or CD4 helper lineages based on their ability to recognize peptide Ags presented by either the MHC class I or class II molecules, respectively. A small fraction of αβ T cells form the NKT cell lineage owing to their TCR selection by lipid Ags presented by CD1d, an MHC-like molecule (1, 2). NKT cells represent a distinct effector group that is capable of providing diverse and fast effector functions and thus is also classified as innate-like T cells (3).

A large fraction of NKT cells use a canonical TCRα-chain resulting from Vα14 to Jα18 rearrangement and are thus named invariant NKT (iNKT) cells (4). The remaining NKT cells, referred to as type II NKT cells, also show highly restricted Vα-Jα usages and recognize lipid Ags different from those recognized by iNKT cells (5–8). iNKT cells share the same developmental history with the rest of αβ T cells up to the double-positive (DP stage) (DP for CD4 and CD8 expression), where the TCRα gene rearranges. Expression and selection of an appropriate TCRα-chain at this stage have been shown to provide the driving force in iNKT cell development (9–11). Most of our understanding of iNKT lineage development is based on events during and after TCRα gene expression at the DP stage. It is not entirely clear whether the highly restricted Vα-Jα usage for NKT cells is simply a result of TCR-mediated selection or additional regulation prior to TCR selection (12, 13).

E proteins and their inhibitors Id proteins have been shown to play important roles at the pre-TCR, the γδTCR, and the αβTCR checkpoints (14, 15). E proteins are basic-HLH motif–containing transcription factors, which bind E-box DNA sequences as dimers (16). Id proteins inhibit E protein function through competitive dimerization with E proteins, thereby preventing E proteins from binding to DNA (17). Two E protein genes, *E2A* and *HEB*, and two Id genes, *Id3* and *Id2*, have been shown to be involved in producing E proteins and Id proteins, respectively, during T cell development (18). Although removal of a single E protein gene only resulted in partial defects in T cell development, deletion of both *E2A* and *HEB* genes in the early stages of T cell development resulted in nearly complete block in αβ lineage development and severe impairment in γδ lineage development (19). Conditional deletion of *E2A* and *HEB* at the DP stage with CD4-Cre also demonstrated an essential role for E proteins in CD4 lineage and iNKT lineage development (20–22). In contrast to E protein gene knockout, deletion of *Id3* early in T cell development resulted in a significant increase in γδ lineage T cells (23), although this increase is almost exclusively restricted to innate-like γδ T cells expressing the Vγ1.1Vδ6.3 TCRs (24). The enhanced γδ lineage development has been attributed to elevated levels of E protein activities because deletion of *Id3* and *E2A* together can correct the innate γδ T phenotype. These genetic studies clearly demonstrated that E protein dosage plays an important role in influencing the fate choice between the γδ and αβ lineages at the pre-TCR and

*Department of Immunology, Duke University Medical Center, Durham, NC 27710; [†]Department of Biomedical Engineering, The University of Texas at Austin, Austin, TX 78712; and [‡]Institute for Cellular and Molecular Biology, The University of Texas at Austin, Austin, TX 78712

Received for publication May 13, 2013. Accepted for publication September 16, 2013.

This work was supported by National Institutes of Health Grants R01GM-059638, R21RR-032742 (to Y.Z.), and K99AG040149 (to N.J.), the Duke University Medical Center Bridge Fund (to Y.Z.), Cancer Prevention and Research Institute of Texas Grant R1120 (to N.J.), and by Welch Foundation Research Grant F1785 (to N.J.).

Address correspondence and reprint requests to Prof. Yuan Zhuang, Department of Immunology, Duke University Medical Center, DUMC-Box 3010, Durham, NC 27710. E-mail address: yzhuang@duke.edu

The online version of this article contains supplemental material.

Abbreviations used in this article: CD1dtet, CD1d tetramer; DN, double-negative; DP, double-positive; iNKT, invariant NKT; PLZF, promyelocytic leukemia zinc finger; SP, single-positive.

γδTCR checkpoints, reminiscent of E protein functions at the αβTCR checkpoint (14, 25).

Given that *Id2* has been shown to collaborate with *Id3* in regulating the TCR checkpoint (22), it is speculated that *Id2* could also collaborate with *Id3* in regulating the pre-TCR and γδTCR checkpoints. In this study, we used Lck-Cre (26) to delete both *Id2* and *Id3* at the pre-TCR and γδTCR checkpoints. Deletion of both *Id2* and *Id3* resulted in a partial block at the pre-TCR checkpoint and increased production of innate γδ T cells, suggesting opposing roles for Id genes in regulating the αβ lineage and the innate γδ lineage. More importantly, analysis of *Id2* and *Id3* double-deficient animals also revealed a novel role for Id2 and Id3 in regulating the development and expansion of iNKT cells. The mutant mice showed a dramatic increase in numbers of iNKT cells. A biased rearrangement involving Vα14-Jα18 was detected in preselecting DP cells, indicating a role for Id proteins in regulating Vα14-Jα18 rearrangement prior to CD1d-mediated selection. Results presented in this study further suggest a dosage-dependent mechanism for Id genes in repressing the fate of innate-like γδ T cells versus iNKT cells during T cell development.

Materials and Methods

Mice

The Lck-Cre transgenic allele (26) and flox alleles for the *Id3* (27), *Id2* (28), *E2A* (26), and *HEB* (19) genes have been previously described. Mice used in this study have been maintained on 129/sv and C57BL/6 mixed background in a specific pathogen-free facility managed by Duke University Division of Laboratory Animal Resources. All procedures have been conducted according to protocols approved by the Institutional Animal Care and Use Committee.

Cell staining and flow cytometry

BrdU staining (BD Biosciences) was performed according to the manufacturer's protocol. Intracellular staining was performed after 2% paraformaldehyde fixation and 0.5% saponin permeabilization. Staining for promyelocytic leukemia zinc finger (PLZF) Ab (provided by Dr. Derek Sant'Angelo) was carried out using a Foxp3 staining buffer set (eBioscience). CD1d tetramers (CD1dtet) with or without loaded PBS57 Ag were obtained from the Tetramer Facility of the National Institutes of Health. CD1d staining was done in dark for 30 min at room temperature before Ab staining of other cell surface markers. FACS was performed on a FACSCanto II (BD Biosciences). Doublets and dead cells were gated out before data analysis. Data were analyzed with FlowJo software (Tree Star).

In vitro OP9-DL1 culture

FACS sorting of double-negative (DN) cells was performed after Dynabead biotin binder (Invitrogen) treatment to deplete CD4 single-positive (SP), CD8 SP, and DP cells. The remaining cells were stained with CD44, CD25, TCRβ, TCRγδ, and CD27 Abs. A mixture of CD4, CD8, Gr-1, Mac-1, B220, and NK1.1 Abs was included in staining as the dump channel to eliminate non-T cells and any residual CD4 SP, CD8 SP, and DP cells. Cells were cultured in MEM-α medium (10% FBS, penicillin/streptomycin, and 5 ng/μl IL-7 for all cultures and additional 5 ng/μl Flt3 ligand for the DN3 culture) on OP9-DL1 cell–coated plates. Lymphocytes were harvested and analyzed by FACS at the specified time points.

V(D)J rearrangement analysis

cDNA from FACS-sorted thymocyte fractions were prepared as described (22). For Vα14-Jα18 usage in CD1dtet-sorted iNKT cells, cDNAs were amplified with primers as described (21, 29). RT-PCR products were subcloned into TOPO TA vector (Invitrogen) and sequenced. Jα gene segment usage was determined using the V-QUEST search program (30) and verified by manual check. For Jα repertoire analysis of DP cells, a Vα8- or Vα14-specific primer and a Cα primer were used to generate libraries for Ion Torrent high-throughout sequencing. Data were converted to the FAST format (31) on a Galaxy platform (http://galaxyproject.org/) before being submitted to the High/V-QUEST search engine (32). A TCRβ V-D-J rearrangement assay was performed with primers Vβ5-5′ and Jβ2.7-3′ according to the protocol described previously (19). Genomic DNA was extracted from FACS-sorted cell fractions.

Results

Conditional removal of Id2 *and* Id3 *with Lck-Cre impairs T cell development*

We hypothesized that *Id2* may play a redundant role and functionally compensate for the loss of function of *Id3* at the pre-TCR checkpoint. To test this hypothesis, we used Lck-Cre to drive conditional deletion of *Id3* and *Id2* before the pre-TCR and γδTCR checkpoints. PCR analysis of fractionated thymocytes demonstrated that Lck-Cre–mediated deletion of the *Id2* and *Id3* floxed alleles started at the DN3 stage and achieved near completion by the DP stage (Supplemental Fig. 1). Mice carrying the Lck-Cre transgene or the floxed alleles alone did not show any phenotype (Supplemental Fig. 2A). Lck-Cre–induced *Id2* deletion alone did not produce any developmental abnormalities, whereas deletion of both copies of *Id3* plus one copy of *Id2* resulted in a dramatic increase in γδ T cells and a reduction in αβ T cells (Fig. 1A, *bottom panel*), a result similar to a previous report of *Id3* knockout mice (23). Deletion of both *Id2* and *Id3* with Lck-Cre (referred to as L-DKO hereafter) resulted in a phenotype significantly different from these control groups. The total thymic cellularity of L-DKO mice was reduced to an average of 36% (among 1.5-mo-old young adults) or 43% (at the weaning age) in comparison with age-matched Cre^- control mice (Fig. 1B). Consistent with an earlier study involving CD4-Cre–mediated deletion of *Id2* and *Id3* at the DP stage, Lck-Cre–mediated deletion of *Id2* and *Id3* at the DN stage also resulted in a complete block in CD8 lineage development (22) (Fig. 1A, *upper panel*). L-DKO mice also exhibited a significant increase in numbers and percentages of $CD4^-CD8^-$ (DN) cells (Fig. 1A, *middle panel*). Further analysis showed that the increase in DN cells could be attributed mostly to a change in the $CD4^-CD8^-CD25^-CD44^-$ (DN4) fraction (from $6.7 \pm 1.1 \times 10^5$ in Cre^- mice to $26.5 \pm 5.2 \times 10^5$ in L-DKO mice; Supplemental Fig. 2B). The absolute numbers of DN3 and DP cells in L-DKO mice were decreased to approximately half of the Cre^- controls (Supplemental Fig. 2B, 2C). Collectively, these results indicated that Lck-Cre induced deletion of Id2 and Id3 perturbed T cell development at multiple stages, including the DN3 stage.

Accumulation of $CD4^-CD8^-TCR\beta^{lo}$ cells occurs during neonatal life

Further examination of L-DKO thymocytes showed that their $CD4^+CD8^-$ cells expressed TCRβ at a level lower than that of CD4 SP in Cre^- controls (Fig. 1C). $TCR\beta^{lo}$ cells were also observed among most $CD4^-CD8^-$ cells and peripheral CD4 T cells in L-DKO mice. Both L-DKO and $Id2^{+/f}Id3^{f/f}$Lck-Cre^+ mice also showed a small fraction of $TCR\beta^-$ cells among the CD4 T cells in the thymus and periphery. A separate FACS analysis showed that these $TCR\beta^-CD4^+CD8^-$ T cells were innate-like γδ T cells as reported in *Id3* knockout mice (24). To uncover the primary developmental defects and to limit the potential cross-regulation from effector T cells generated in the mutant mice, we switched to examination of neonatal animals (Fig. 1D). Among day 3 neonates, CD4 cells were not detected in L-DKO mice, indicating a developmental block in the transition from DP to CD4 SP. $CD4^-CD8^-TCR\beta^{lo}$ T cells were also absent at this early stage. In contrast, a dramatic increase in $CD4^-CD8^-TCR\beta^{lo}$ T cells and γδ T cells became apparent 10 d after birth concomitant with the appearance of CD4 cells. By day 20 (weaning age), both $CD4^-CD8^-TCR\beta^{lo}$ T cells and CD4 cells exhibited a further increase in percentages relative to other populations in the thymus of L-DKO mice. CD4 cells in the mutant mice expressed a lower level of TCRβ in comparison with the CD4 cells in the Cre^- control mice

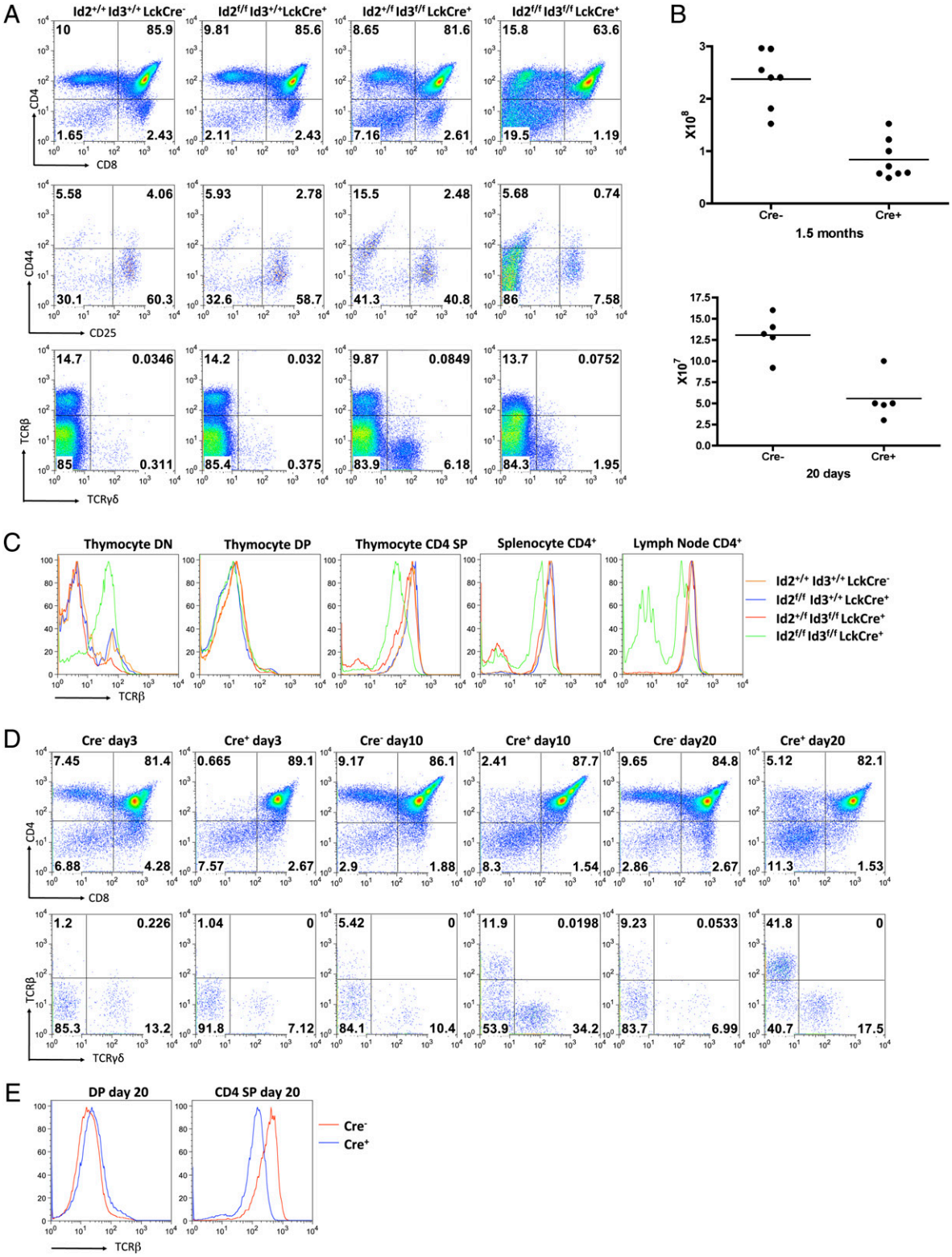

FIGURE 1. Early T cell development is perturbed by Lck-Cre–induced knockout of *Id2* and *Id3*. (**A**) Total thymocytes were analyzed in two-dimensional plots of either CD4 and CD8a (*top panel*) or TCRβ and TCRδ (*bottom panel*). The DN fractions (defined by $CD4^-CD8^-NK1.1^-B220^-Gr\text{-}1^-Mac\text{-}1^-$) of thymocytes were displayed by CD44 and CD25 expression (*middle panel*). Samples are from 2-mo-old $Id2^{+/+}Id3^{+/+}LckCre^-$, $Id2^{f/f}Id3^{+/+}LckCre^+$, $Id2^{+/f}Id3^{f/f}LckCre^+$, and $Id2^{f/f}Id3^{f/f}LckCre^+$ mice as indicated on the top of each column. Percentages of cells in each quadrant are displayed. (**B**) Cell counts of total thymocytes in 1.5-mo-old and 20-d-old mice. The mean value for 1.5-mo-old Cre^- control mice is $2.4 \pm 0.2 \times 10^8$ ($n = 7$), and for Cre^+ L-DKO mice is $0.85 \pm 0.13 \times 10^8$ ($n = 8$). The p value of the t test between the two groups is <0.0001. The mean value for 20-d-old Cre^- control mice is $13 \pm 1.1 \times 10^7$ ($n = 5$), and for Cre^+ L-DKO is $5.6 \pm 1.2 \times 10^7$ ($n = 5$). The p value of the t test between the two groups is 0.0017. (**C**) Expression level of TCRβ among indicated cell fractions isolated from thymus, spleen, and lymph nodes. (**D**) FACS analysis of day 3, 10, and 20 neonatal Cre^- and $Cre^+Id2^{f/f}Id3^{f/f}$ thymocytes. Plots shown are CD4/CD8a staining of total thymocytes (*top panel*) and TCRβ/TCRδ staining of DN fractions (*bottom panel*). Percentages of cells in each quadrant are shown. Results are representative of three Cre^- and Cre^+ pairs at each time point. (**E**) Cre^- (red) and Cre^+ (blue) samples from day 20 shown in (D) were further analyzed in an overlay histogram to display TCRβ expression in DP and CD4 SP cells.

(Fig. 1E). Based on these findings, we chose 20-d-old animals to further dissect T cell development in L-DKO mice.

A partial block at the pre-TCR checkpoint

Given that Lck-Cre initiates *Id2* and *Id3* deletion at the DN3 stage, we first evaluated the effect of Id deletion on pre-TCR selection. We used CD27 to separate DN3 cells into DN3a ($CD27^{lo}$) and DN3b ($CD27^{hi}$) fractions (Fig. 2A). CD27 upregulation is tightly correlated with pre-TCR selection among DN3 cells (33). Analysis of L-DKO mice showed that the percentage of DN3b cells within the DN3 fraction was reduced to approximately one-half of that in Cre^- control littermates (Fig. 2B). To determine whether this block in pre-TCR selection was due to any major perturbations of TCRβ gene rearrangement, we examined TCRβ gene usage based on V-D-J rearrangements (19). A random pattern of Jβ usage was detected among DN3 and DN4 cells in Cre^- mice and DN3 cells from L-DKO mice (Fig. 2C). This result indicated a relatively normal TCRβ usage among DN3 cells in L-DKO mice. However, both $CD4^-CD8^-TCR\beta^+$ and $CD4^-CD8^-TCR\beta^-$ cells in L-DKO mice showed a perturbed pattern of D-J usage.

To further evaluate the efficiency of pre-TCR selection, we tested the differentiation capability of DN3 cells in an OP9-DL1 culture system (34). DN3 cells from both Cre^- control and L-DKO samples expanded dramatically and differentiated into the DP stage within 6 d in culture (Fig. 2D, 2E). However, DN3a cells from L-DKO mice progressed from DN to DP in a slower kinetics in comparison with the Cre^- controls (Fig. 2D). The kinetic difference between these two genotype groups was also evident among the sorted DN3b cells (Fig. 2E), which represents cells having undergone β-selection (33). Collectively, these data indicate that

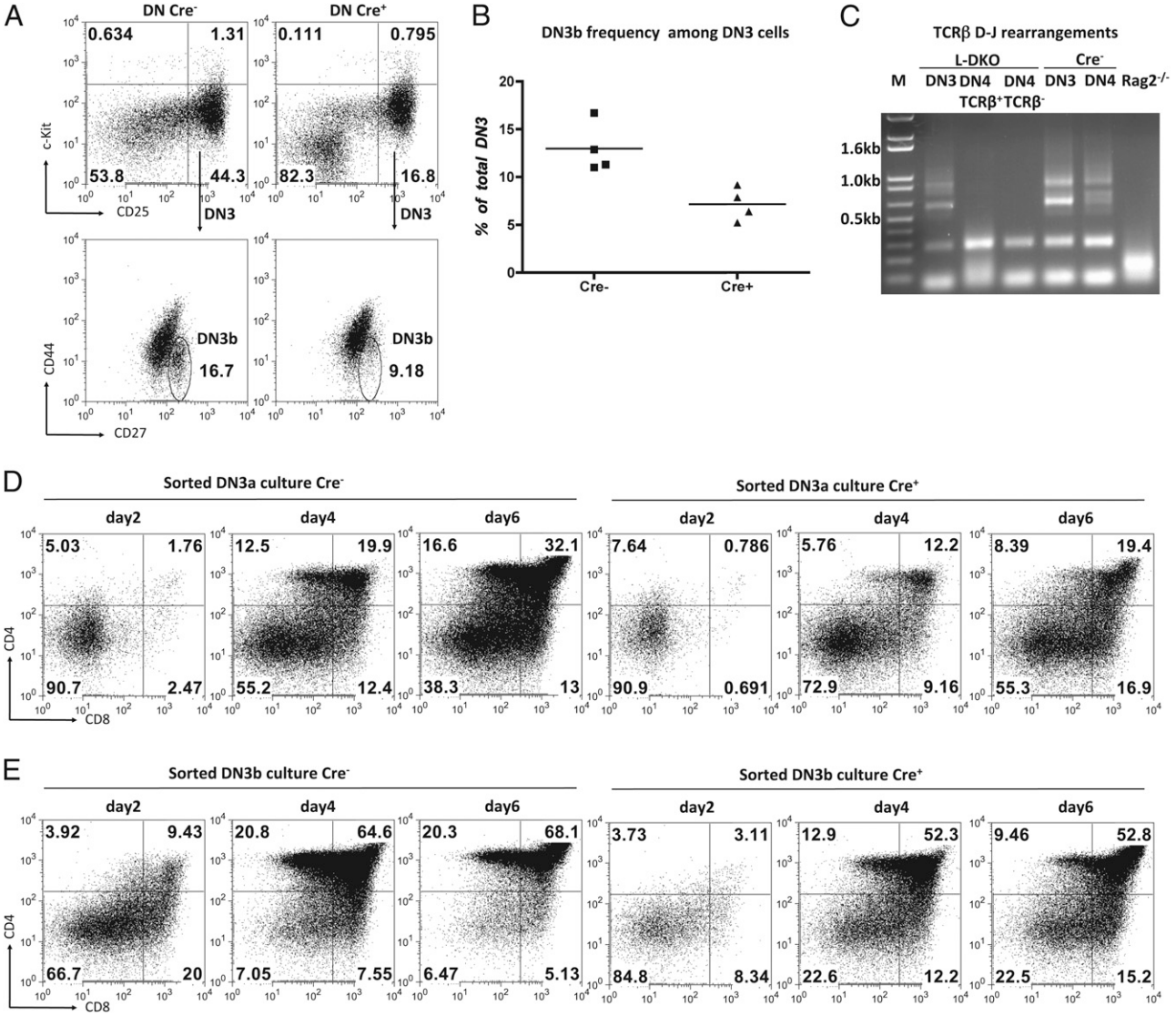

FIGURE 2. Pre-TCR checkpoint is partially blocked. (**A**) Separation DN3a and DN3b fractions with CD27 marker. DN cells were defined as $CD4^-CD8^-NK1.1^-B220^-Gr\text{-}1^-Mac\text{-}1^-$ here in FACS sorting. DN3 fraction was first gated as a $c\text{-}Kit^-CD25^+$ fraction of DN thymocytes before analysis with CD44 and CD27. (**B**) Summary of DN3b percentages in total DN3 from four independent sortings. Means ± SE are 13 ± 1.3% for Cre^- and 7.2 ± 0.86% for Cre^+ samples with $p = 0.01$. (**C**) TCRβ D-J rearrangement assay with Vβ5 and Jβ2.7 primers. Lane orders are: M, size marker; L-DKO DN3; L-DKO DN4 $TCR\beta^+$; L-DKO DN4 $TCR\beta^-$; Cre^- DN3; Cre^- DN4; $Rag2^{-/-}$. The predicted size for each rearrangement is: Jβ2.7, 282 bp; Jβ2.6, 495 bp; Jβ2.5, 638 bp; Jβ2.4, 730 bp; Jβ2.3, 869 bp; Jβ2.2, 1135 bp; Jβ2.1, 1338 bp. (**D**) OP9-DL1 culture of DN3a thymocytes sorted from Cre^- controls (*left panel*) and L-DKO mice (*right panel*). Twenty thousand cells were seeded in each well for the time course experiments. CD4 and CD8 staining of total cultured cells are shown for days 2, 4, and 6 in culture. Results are representative of three repeats of independently sorted cells. (**E**) OP9-DL1 culture of DN3b thymocytes sorted from Cre^- controls (*left panel*) and L-DKO mice (*right panel*). Four thousand cells were seeded in each well for the time course experiments. Analysis was carried out as described in (D). Results are representative of three repeats of independently sorted cells.

Lck-Cre–mediated deletion of *Id2* and *Id3* impaired the pre-TCR checkpoint.

$CD4^+CD8^-TCR\beta^{lo}$ and $CD4^-CD8^-TCR\beta^{lo}$ cells in L-DKO mice are mostly iNKT cells and type II NKT cells

iNKT cells are known to express lower levels of TCR than those of conventional αβ T cells and are phenotypically classified into either the $CD4^+CD8^-$ or $CD4^-CD8^-$ compartment. The development of iNKT cells also begins in the neonatal stage (4) with a time frame similar to the $CD4^+CD8^-TCR\beta^{lo}$ cells and $CD4^-CD8^-TCR\beta^{lo}$ cells in L-DKO mice. We therefore examined the possibility that the $TCR\beta^{lo}$ cells in L-DKO mice were iNKT cells. FACS analysis of thymocytes revealed that most $CD4^+$ cells and a third of $CD4^-CD8^-$ cells in L-DKO mice were recognized by an Ag-loaded CD1dtet that specifically binds to the canonical TCR on iNKT cells (Fig. 3A). PLZF has been shown to be a signature transcription factor for innate T lymphocytes, including Vγ1.1Vδ6.3 γδ T cells and iNKT cells (35). Intracellular staining with anti-PLZF Ab demonstrated an overall increased expression of PLZF in $CD4^+CD8^-$ and $CD4^-CD8^-$ cells but not DP cells in L-DKO mice (Fig. 3B). PLZF expression was found in both $\alpha\beta^+$ and $\gamma\delta^+$ fractions of $CD4^-CD8^-$ cells in the mutant mice. Furthermore, a small fraction of $TCR^-CD4^-CD8^-$ cells also expressed PLZF, indicating their possible lineage relationship with TCR^+ PLZF-expressing cells. On average, the absolute numbers of CD4 SP and DN fractions in L-DKO mice were ~9- and 28-fold higher, respectively, than those of the age-matched Cre^- controls (Fig. 3C). Because most CD4 SP and DN fractions in L-DKO mice expresses PLZF, we conclude that *Id2* and *Id3* double deletion leads to a significant increase in numbers of PLZF-expressing thymocytes. Sequencing analysis of cDNA products amplified with Vα14- and Jα18-specific primers confirmed the exclusive usage of the canonical invariant Vα14Jα18 TCR in CD4 $CD1dtet^+$ cells isolated from L-DKO mice (Fig. 3D).

The lipid Ag used in the CD1dtet specifically recognizes iNKT cells. Type II NKT cells have been shown to use several highly restricted VαJα rearrangements, including Vα3 to Jα9 rearrangement (7, 8). Therefore, we examined Vα3Jα9 usage in the $TCR\beta^{lo}CD1dtet^-$ $CD4^-CD8^-$ and $CD4^+CD8^-$ cells in the mutant mice. Vα3Jα9 products but not Vα14Jα18 products were readily detected by PCR in $TCR\beta^{lo}CD1dtet^-$ cells (Fig. 3E). Sequence analysis of Vα3Jα9 products from $TCR\beta^{lo}CD1dtet^-$ cells indicated that a third of them were in-frame and the remaining two-thirds were out-of-frame Vα3Jα9 rearrangements (Fig. 3F). Therefore, other Vα rearrangements must also be involved in generating functional TCRα-chains in the $TCR\beta^{lo}CD1dtet^-$ fraction.

To further test lineage identity of the expanded TCR^{lo} cells in L-DKO mice, we bred L-DKO mice to the MHC class II–deficient background. Both $TCR\beta^{lo}CD1dtet^+$ and $TCR\beta^{lo}CD1dtet^-$ cells in L-DKO mice were generated in the absence of MHC class II selection (Fig. 4), demonstrating that these cells were unrelated to the conventional helper T cell lineages. Thus, we conclude that Lck-Cre–mediated deletion of *Id2* and *Id3* resulted in increased generation of both iNKT cells and type II NKT cells.

Expansion of stage 1 iNKT cells in L-DKO mice

Further analysis showed that most iNKT cells developed in L-DKO mice do not express NK1.1 and DX5 even though they have downregulated CD24 (Fig. 5A). FACS analysis also showed that iNKT cells in L-DKO mice expressed low levels of CD44 (Fig. 1A). These features together with PLZF expression indicated that iNKT cell development in L-DKO mice has progressed to stage 1 (36, 37), where cells undergo proliferative expansion (38). Indeed, in vivo BrdU pulse labeling revealed a significantly higher fraction of cycling cells among $CD4^+$ population in L-DKO mice (most of which are iNKT cells) in comparison with the conventional CD4 SP cells in Cre^- controls (Fig. 5B, 5C). The percentage of cycling cells was also higher in the DN TCR^{lo} fraction of L-DKO mice (most of which are presumed type II NKT cells) in comparison with the conventional CD4 SP cells in Cre^- controls. The same analysis indicated a relative normal pattern of cell cycle for L-DKO mice at the DN2, DN3, and DP stages of T cell development (Fig. 5C, Supplemental Fig. 3). This proliferative behavior of NKT cells was observed at both weaning and young adult age (Fig. 5B). Repertoire analysis with a panel of TCR Vβ isotype-specific Abs revealed a broad pattern of Vβ usage among $CD4^+$ cells of L-DKO mice, indicating that the expanded iNKT cells in L-DKO mice remain polyclonal (Table I). However, the overall patterns of Vβ usage in L-DKO mice were different from the conventional Vβ8 > Vβ7 > Vβ2 rule (39), indicating the possibility of an altered selection during development or expansion phase of these iNKT cells. Furthermore, five of six L-DKO mice showed increased Vβ usage involving Vβ8.3, Vβ11, or Vβ13. Taken together, these results indicated that *Id2* and *Id3* deletion resulted in an expansion of immature iNKT cells.

Id2 *and* Id3 *deletion results in a biased rearrangement toward Vα14-Jα18*

Given that iNKT cell development is dependent on Vα14 to Jα18 rearrangement, which typically occurs during the DP window of thymocyte development, we asked whether *Id2* and *Id3* deletion affects TCRα rearrangement. We assessed the Jα usage by performing high-throughput sequencing of rearrangement products involving either Vα8 or Vα14 genes from the preselecting $CD4^+CD8^+CD69^-$ DP cells. $CD1dtet^+$ and $CD69^+$ postselecting cells were gated out to avoid the contamination of NKT cells or mature αβ T cells (Supplemental Fig. 4). Jα usage was captured by PCR amplification with a Vα-specific primer and a Cα primer. A broad pattern of Jα usage involving Vα8 rearrangements was detected in both Cre^- control and L-DKO cells (Fig. 6A). Because Vα8 is one of the commonly used Vα genes (40), the random distribution of Jα usage indicates that a significant fraction of DP cells undergoes relatively normal TCRα rearrangements. In contrast to the Vα8 result, Vα14 rearrangements exhibited a highly skewed pattern toward Jα18 usage in L-DKO mice (Fig. 6B). This bias toward Jα18 was associated with Vα14 but not Vα8 (Fig. 6A). It remains a possibility that some of these Vα14-Jα18 rearrangements may come from NKT cells that have downregulated their surface TCR. However, this argument cannot fully explain the fact that a significant number of unproductive Vα14-Jα18 rearrangements were also observed in three independent L-DKO DP samples (18, 19, and 61%; Fig. 6B, *lower panel*). In particular, one of the three samples (Fig. 6B, *center pie chart*) showed more unproductive rearrangements (61%) than productive rearrangements (37%), which presents a typical preselecting repertoire. In contrast, unproductive Vα14-Jα18 rearrangements were detected at a much lower frequency in three wild-type control samples (0, 0.01, and 5%; Fig. 6B, *upper panel*). This result suggests that *Id2* and *Id3* deletion promotes Vα14 to Jα18 rearrangements among developing T cells when Vα14 is involved in rearrangements.

Increased iNKT development in Id2- and Id3-deficient mice is driven by high levels of E proteins

The major targets of Id proteins are E protein transcription factors, although E proteins are not the only Id-interacting proteins reported thus far (41). To test whether enhanced iNKT development is indeed regulated by E proteins, we lowered the E protein dosage by removing one copy each of the *E2A* and *HEB* genes on

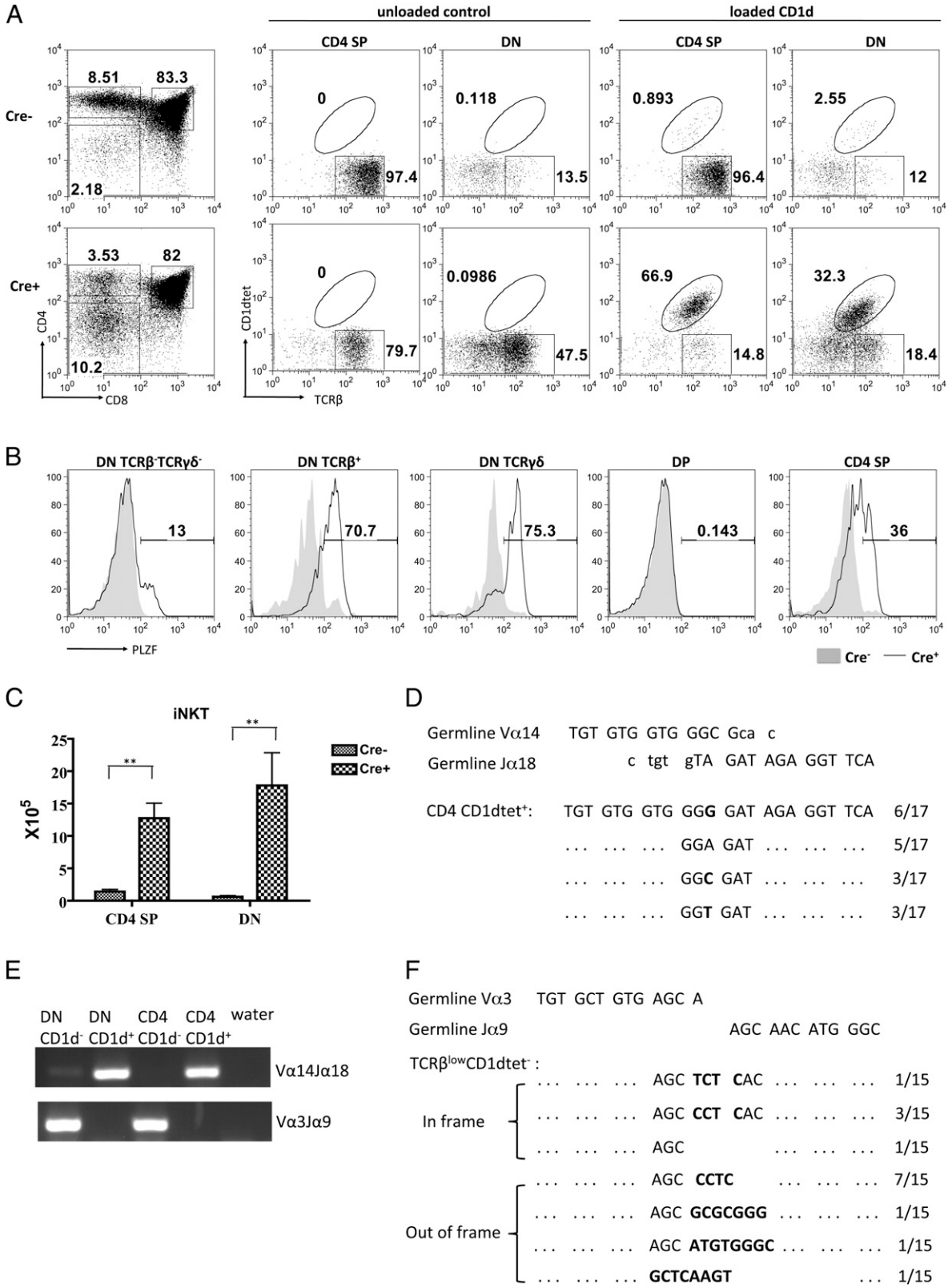

FIGURE 3. $CD4^-CD8^-TCR^{lo}$ and $CD4^+CD8^-TCR^{lo}$ cells in L-DKO mice are NKT cells. (**A**) Representative staining of total lymphocytes with CD4, CD8, TCRβ, and CD1dtet. CD4 and CD8 staining of total thymocytes were used to define DN and CD4 SP gates. DN and CD4 fractions of each genotype were analyzed with either unloaded CD1dtet as a control or PBS57-loaded CD1dtet. The percentages of $CD1dtet^+$ or $TCR\beta^+CD1dtet^-$ cells in CD4 and DN fractions are displayed in the plots. (**B**) Intracellular staining of PLZF in CD4 SP ($CD4^+CD8^-$), DP ($CD4^+CD8^+$), and DN ($CD4^-CD8^-$) fraction of total lymphocytes. DN fraction is further separated by TCRβ and TCRδ. DN $TCR\beta^-TCR\delta^-$, DN $TCR\beta^{lo}$, and DN $TCR\delta^+$ populations were analyzed. (**C**) Cell counts for $CD1dtet^+$ iNKT cells in CD4 SP and DN fractions in 20-d-old pups. The mean values for CD4 SP iNKT cells are $1.43 \pm 0.31 \times 10^5$ and $12.76 \pm 2.34 \times 10^5$ in Cre^- controls and L-DKO, respectively, with $p = 0.0013$. The mean values for DN iNKT cells are $0.64 \pm 0.15 \times 10^5$ and $17.81 \pm 5.08 \times 10^5$ in Cre^- controls and L-DKO, respectively, with $^{**}p = 0.0097$. Five mice of each genotype group were used in the analysis. (**D**) Sequence results of Vα14Jα18 junctions from cDNA of DN $CD1dtet^+$ and CD4 $CD1dtet^+$ populations in L-DKO mice. N additions are shown in (*Figure legend continues*)

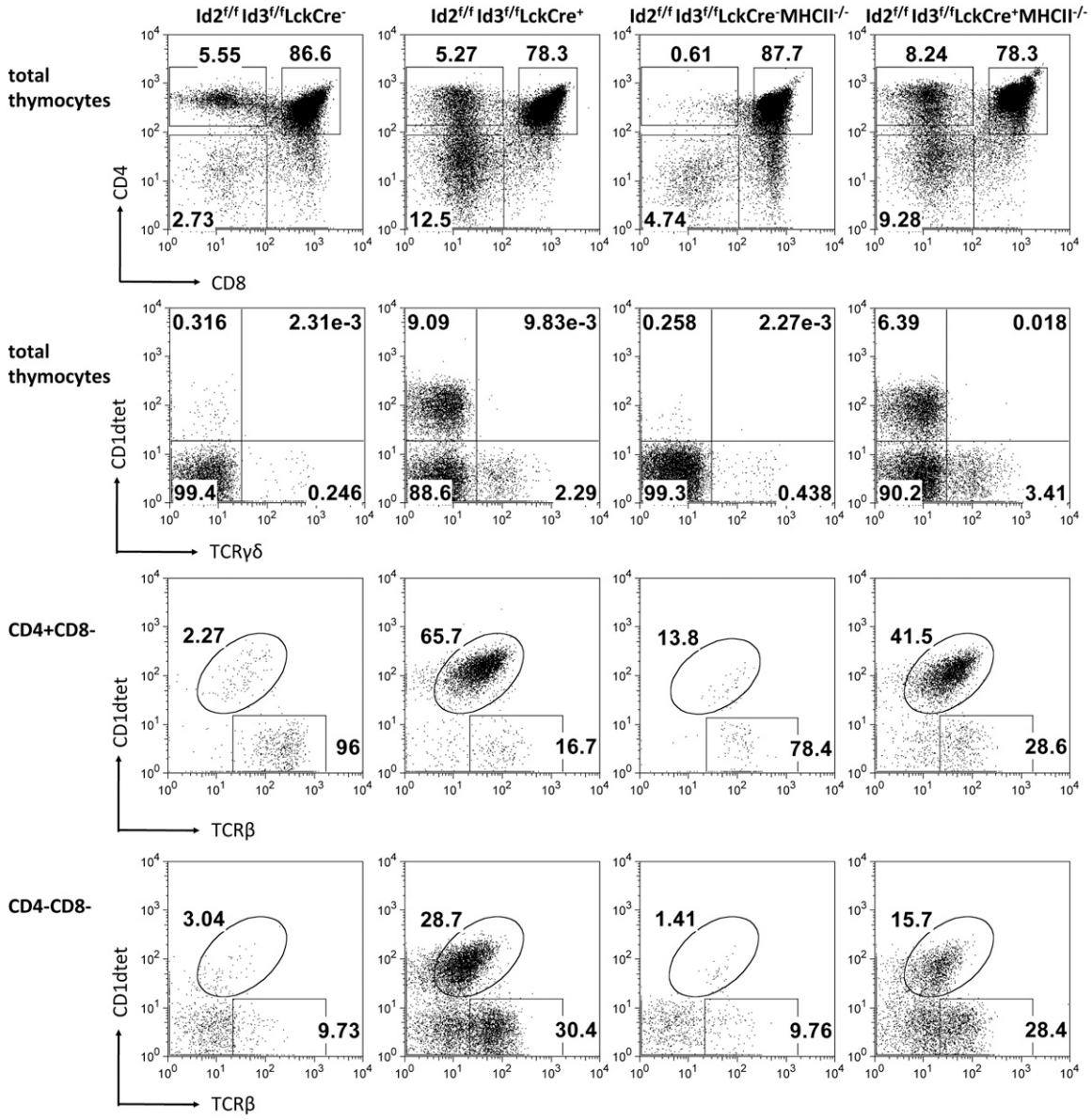

FIGURE 4. Development and expansion of iNKT cells in L-DKO mice is independent of MHC class II. Total thymocytes were analyzed with either CD4 and CD8a (*first row across*) or CD1dtet and TCRγδ (*second row across*) staining. The $CD4^+CD8^-$ (*third row across*) and $CD4^-CD8^-$ (*fourth row across*) fractions of thymocytes were displayed by CD1dtet and TCRβ expression. Samples are from 20-d-old $Id2^{f/f}Id3^{f/f}LckCre^-$, $Id2^{f/f}Id3^{f/f}LckCre^+$, $Id2^{f/f}Id3^{f/f}LckCre^-$MHC class $II^{-/-}$, and $Id2^{f/f}Id3^{f/f}LckCre^+$MHC class $II^{-/-}$ mice as indicated on the top of each column. Percentages of cells in each quadrant are displayed. $n = 2$ for each genotype.

the L-DKO background (referred to as L-DKO50%E). This genetic change effectively reduced iNKT cell numbers almost back to the level seen in Cre^- controls and concurrently enhanced numbers of γδ T cells dramatically (Fig. 7A, 7B). Further analysis confirmed that the expanded γδ T cells in L-DKO50%E mice belong to the innate γδ T lineage that uses exclusively the Vδ6.3 TCR (Fig. 7A, *right panel*). This result indicates that innate γδ T and iNKT lineages are regulated by different levels of E proteins. To further evaluate the necessity of E proteins in the generation of innate γδ T cells, we generated $Id2^{f/f}Id3^{f/f}E2A^{f/f}HEB^{f/f}$Lck-$Cre^+$ quadruple-deficient mice (referred to as L-QKO mice). Deletion of *E2A* and *HEB* effectively prevented αβ T and iNKT lineage development (Fig. 7C). Numbers of γδ T cells in L-QKO mice were also reduced to 10% of the Cre^- controls (Fig. 7D), a phenotype similar to the previously defined Lck-Cre–mediated *E2A* and *HEB* knockout mice (19). This result demonstrated that the *Id2* and *Id3* genes control iNKT lineage development through inhibition of E protein activities exclusively.

Discussion

Following a recent publication demonstrating an essential role for *Id3* and *Id2* at the TCR selection checkpoint (22), the present study provided new genetic evidence that *Id2* and *Id3* are also collectively involved in regulating the pre-TCR checkpoint. Furthermore, our

bold. (**E**) PCR analysis of Vα14Jα18 and Vα3Jα9 rearrangement in $CD1dtet^+$ and $CD1dtet^-$ fraction of DN and CD4 cells. Results are representative of two independent experiments involving separate L-DKO mice. (**F**) Sequence results of Vα3Jα9 junctions from cDNA of $TCR\beta^{lo}CD1dtet^-$ population in L-DKO mice. N additions are shown in bold.

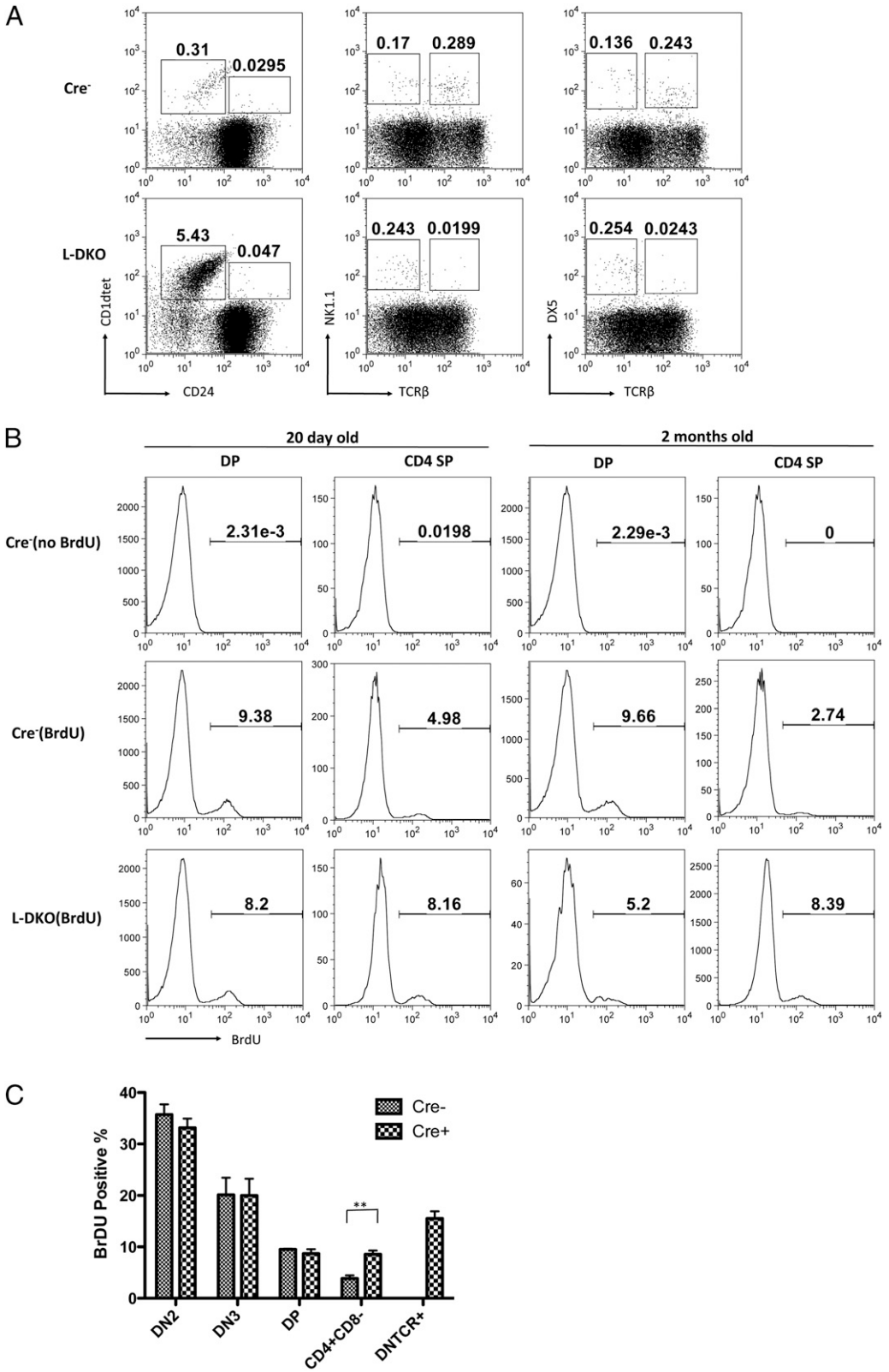

FIGURE 5. Characterization of NKT cells in L-DKO mice. (**A**) Total thymocytes from Cre$^-$ control L-DKO mice were displayed for CD1dtet and CD24 expression (*left column*), NK1.1 and TCRβ expression (*middle column*), and DX5 and TCRβ expression (*right column*). (**B**) BrdU incorporation among DP and CD4$^+$ SP thymocytes analyzed at 4 h after BrdU injection of 20-d-old (*left panel*) or 2-mo-old mice (*right panel*). The percentage of BrdU$^+$ cells for each subpopulation is shown in histograms. (**C**) Summary of BrdU$^+$ percentages in DN2, DN3, DP, CD4$^+$CD8$^-$, and DN TCRβ$^+$ fractions from three independent experiments of 20-d-old pups. Significant difference was observed between L-DKO and control mice among the CD4$^+$CD8$^-$ fraction (mean value, 3.85 ± 0.61 and 8.56 ± 0.72% for Cre$^-$ controls and L-DKO, respectively, with $^{**}p = 0.0076$). Numbers of DN TCR$^+$ cells in the Cre$^-$ control group were too small to be included in this analysis.

Table I. TCR Vβ repertoire analysis of L-DKO $CD4^+$ thymocytes

Mouse Strain	Vβ2	Vβ3	Vβ4	Vβ5.1/5.2	Vβ6	Vβ7	Vβ8.1/8.2	Vβ8.3	Vβ9	Vβ10[b]	Vβ11	Vβ12	Vβ13
Cre^- (LIIIV49) 1m	1.45	3.15	4.96	5.91	8.11	2.51	7	3.44	0.37	1.87	3.79	3.23	1.16
Cre^- (LIIV41) 1.5m	3.12	2.87	5.22	7.33	7.57	2.96	8.64	4.54	0.89	2.92	4.5	3.53	1.4
Cre^- (LIIIV25) 2m	1.45	2.76	5.21	4.8	7.83	4.1	7.04	4.74	0.47	2.14	3.56	2.66	1.42
	3.94	3.62	6.8	5.23	7.53	2.99	9.79	5.09	0.78	3.66	5.39	4.26	1.93
B6 2m	3.78	3.86	7.26	5.2	7.6	2.73	9.5	4.82	0.97	3.69	4.73	3.63	1.74
Average ± SD	2.75 ± 1.22	3.25 ± 0.48	5.89 ± 1.06	5.69 ± 1.00	7.73 ± 0.24	3.06 ± 0.61	8.39 ± 1.32	4.53 ± 0.64	0.70 ± 0.26	2.86 ± 0.84	4.39 ± 0.74	3.46 ± 0.58	1.53 ± 0.30
L-DKO (LIIIV24) 2m	2.01	2.67	2.54	2.94	3.23	4.48	4.36	18.2	2.29	2.48	8.13	2.96	3.04
L-DKO (LIIIV26) 2m	0.60	1.16	0.63	3.74	1.78	4	7.31	2.04	0.25	0.56	12.7	0.68	4.15
L-DKO (LIIIV17) 2m	1.61	2.06	1.86	2.47	3.05	4.19	6.57	7.87	1.45	1.76	27	2.61	10.8
L-DKO (LIIIV47) 1m	0.99	0.79	1.83	2.06	1.98	3.32	10.7	2.45	1.39	0.93	9.91	0.90	8.44
L-DKO (LIIIV48) 1m	1.32	1.05	0.99	2.47	4.22	4.13	11.7	2.49	0.62	0.70	3.65	0.95	3.34
L-DKO (LIIIV50) 1m	0.28	0.68	0.72	2.55	2.9	3.33	14.5	3.29	1.18	1.16	2.84	0.66	10.9
Average ± SD	1.14 ± 0.64	1.40 ± 0.79	1.43 ± 0.76	2.71 ± 0.58	2.86 ± 0.89	3.91 ± 0.48	9.19 ± 3.76	6.06 ± 6.33	1.20 ± 0.71	1.27 ± 0.73	10.71 ± 8.81	1.46 ± 1.04	6.78 ± 3.71

Frequencies of Vβ usage are shown as percentages among $CD4^+CD8^-$ fraction of thymocytes isolated from five control mice and six L-DKO mice. The average and SD are calculated for each group. Numbers in parentheses are identifiers of the mice used in the experiment. Abs used in the analysis are from a TCR Vβ screening panel from BD Pharmingen.
m, Mouse age in months.

study also revealed a previously unanticipated role for *Id3* and *Id2* in regulating iNKT cell development.

Two models have been proposed to explain the development of iNKT cells (13). The "pre-commitment" model postulates that iNKT cell fate is predetermined prior to CD1d-mediated selection. This idea has been supported by the finding that Vα14-Jα18 rearrangements can be detected prior to the appearance of conventional αβ T cells in the mouse fetus (12). However, this finding is inconsistent with the fact that most Vα14-Jα18 rearrangements occur as secondary rearrangements in DP cells, from which iNKT cells are generated continuously in postnatal life (9–11). The "mainstream" (or TCR-instructive) model argues that iNKT cells acquire their lineage identity upon CD1d-mediated TCR selection of DP cells that have successfully produced the canonical Vα14-Jα18 TCR resulting from the sequential rearrangement of the TCRα gene segments. Recent studies further demonstrated that a strong TCR signal is associated with activation of NKT lineage-specific transcription factors such as PLZF (42). Mounting evidence supports the idea that CD1d-mediated selection, together with signaling events involving the SLAM receptors, drive iNKT lineage differentiation (37). In light of these previous findings, our observation of a biased Vα14-Jα18 rearrangement in L-DKO mice provides an alternative view to the existing models. We propose that Vα14-Jα18 rearrangement is not a random event and is subject to repression by concerted activity of Id3 and Id2.

Multiple factors may contribute to the overall increase in numbers of iNKT cells in L-DKO mice. The Jα repertoire analysis of L-DKO DP cells clearly revealed a biased usage of Vα14-Jα18 when Vα14 is used in rearrangement. Because Jα18 usage was not altered when Vα8 was used in rearrangements, the biased Vα14-Jα18 rearrangement in D-LKO mice cannot be simply due to targeted regulation at the Jα18 site. Given that each Vα gene is regulated by an independent promoter, we propose that Vα14 may be subject to targeted regulation in L-DKO mice. However, Vα14 must be working in concert with Jα18 in L-DKO mice to promote Vα14-Jα18 usage. This biased Vα14-Jα18 usage may only affect a small fraction of DP cells because the pattern of Vα8 rearrangements, a relatively common Vα, seems unperturbed in L-DKO mice. Therefore, altered Vα14-Jα18 usage alone is not sufficient to explain the overall increase in iNKT cell numbers. Our study has further revealed that most iNKT cells detected in the thymus of L-DKO mice are proliferating immature iNKT cells. The expansion of immature iNKT cells after TCRα rearrangement could be another reason for the increase of iNKT cells in L-DKO mice.

The expansion of iNKT cells in L-DKO mice could also be attributed to other T lineage cells developing along with iNKT cells that may inadvertently affect the development and expansion of iNKT cells (43). These include the innate γδ T cells that developed in the neonatal stage and the small number of conventional CD4 SP cells made through positive selection (22). Indeed, CD4 SP cells that developed in Id3-deficient background have been shown to exhibit various effector phenotypes (44), which could potentially influence the development and expansion of iNKT cells. To resolve this issue, we have tested our L-DKO mice on an MHC class II–deficient background and observed a similar expansion of iNKT cells as in L-DKO mice. The effect of innate γδ T cell on the development of iNKT cells in our L-DKO model could be further investigated in the future by crossing the L-DKO mice to the TCRδ-deficient background.

Under our experimental conditions, the innate γδ lineage and iNKT lineage are selectively expanded in response to increasing levels of E proteins. The tight correlation between E protein dosage and unique TCR types such as Vγ1.1Vδ6.3 of innate γδ T cells and Vα14Jα18 of iNKT cells provides a genetic frame-

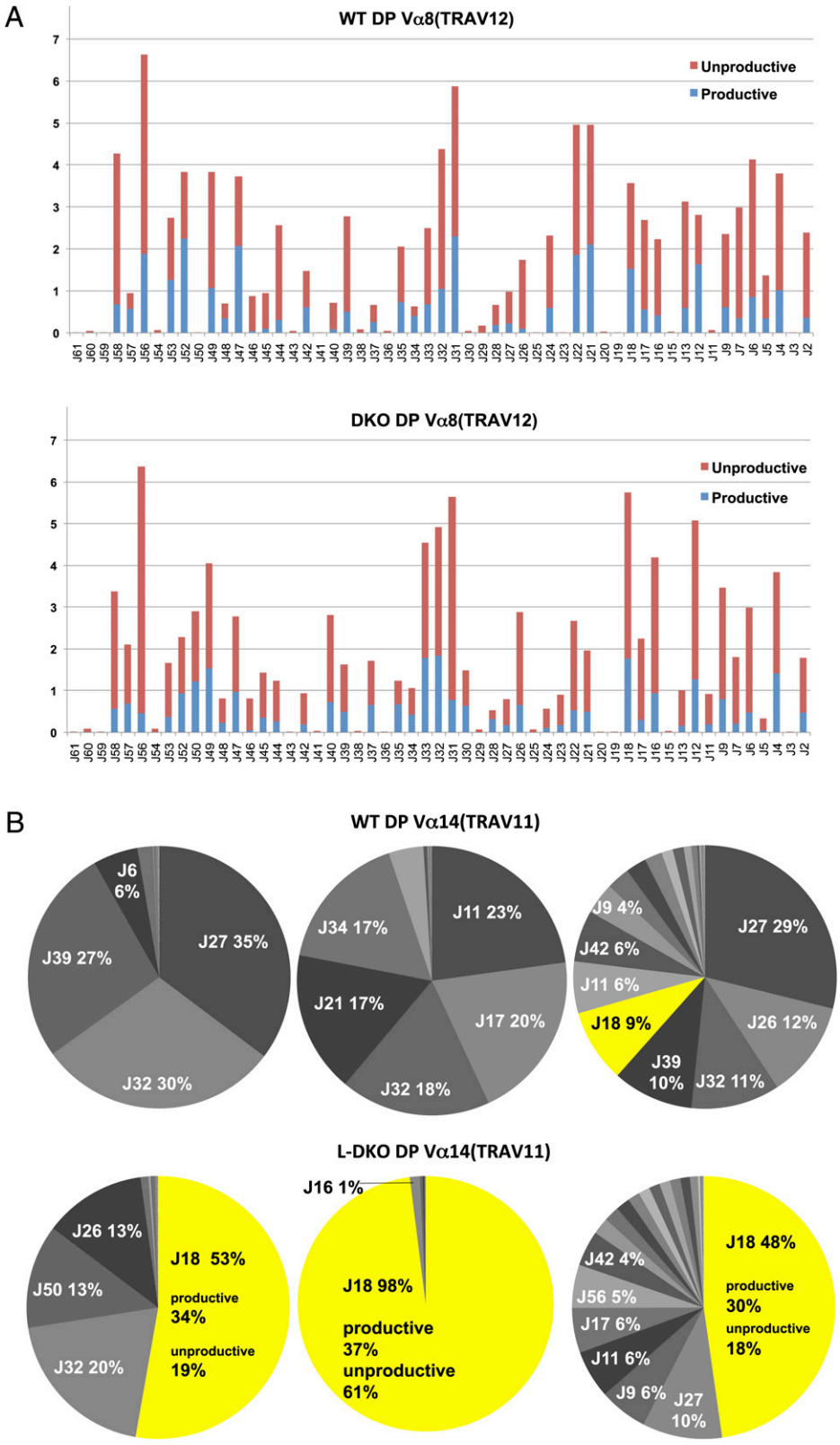

FIGURE 6. Jα repertoire analysis of DP cells. (**A**) Jα repertoire analysis of Vα8-Cα PCR products amplified from a Cre$^-$ control (*top*) and L-DKO (*bottom*) CD69$^-$ DP cells. Bar graphs depict relative percentages of each Jα gene usage separated by productive and unproductive rearrangements. Jα genes are shown according to their relative positions in the TCRα locus starting with the Vα-proximal Jα61 gene. Analysis was based on 24,124 and 17,482 sequence reads for Cre$^-$ control and L-DKO cells, respectively. (**B**) Jα repertoire analysis of Vα14-Cα PCR products amplified from a Cre$^-$ control (*top*) and L-DKO (*bottom*) CD69$^-$ DP cells. Each pie chart represents result of a single animal. The relative percentages of J gene usage were depicted in shaded slices with Jα18 highlighted in yellow. Sequence reads were 37,811, 10,994, and 7,468 for wild-type samples and 37,758, 46,141, and 7,960 for mutant samples.

work for further understanding how TCR rearrangement, expression, and signaling are coupled with E protein–mediated lineage differentiation programs.

Investigation of PLZF expression shed new light on the lineage relationship between Vγ1.1Vδ6.3 γδ T cells and iNKT cells (45, 46). Although these two innate lineages seem to be developed independently during thymopoiesis, they clearly share a similar developmental blueprint by employing PLZF-mediated transcriptional regulation and possess similar innate-like features such as restricted TCR usage, acquisition of effector memory like phenotypes upon maturation, and coexpression of IL-4 and IFN-γ (35). Furthermore, a recent RNA expression profiling analysis classified iNKT cell as a lineage closely related to γδ T cells (47). This result supports the idea that NKT cells could be evolutionarily

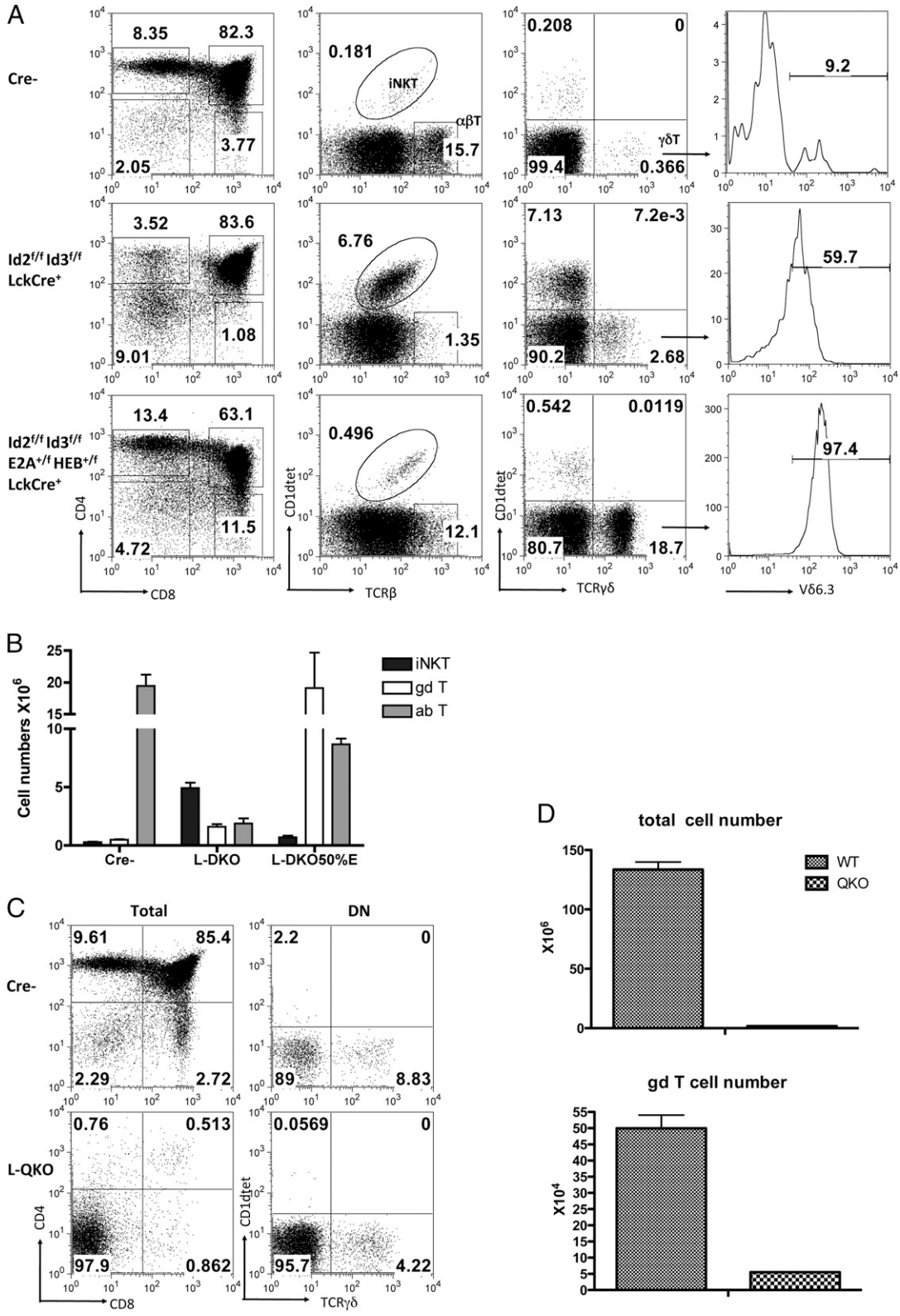

FIGURE 7. E protein dosages at the DN3 stage control lineage outcomes. (**A**) Effects of E protein dosage on T cell development revealed by analysis of Cre$^-$ control, L-DKO, and L-DKO50%E (Id2$^{f/f}$Id3$^{f/f}$E2A$^{+/f}$HEB$^{+/f}$Lck-Cre$^+$) mice. Total thymocytes were analyzed with either CD4 and CD8 staining (*far left column*), CD1dtet and TCRβ staining (*middle left column*), or CD1dtet and TCRδ staining (*middle right column*). TCRδ$^+$ cells were further analyzed for Vδ6.3 expression (*far right column*). (**B**) Cell counts of each T cell fractions as defined in (A). Three mice for each genotype group were included in the analysis. (**C**) FACS analysis of L-QKO mice. Results of CD4 and CD8 analysis of total thymocytes (*left column*) are shown along with the CD1dtet and TCRβ analysis of gated DN fractions (*right column*). Results are representative of three pairs of animals. (**D**) Cell counts for total thymocytes (*top*) and γδ T cells (*bottom*) in the thymus of 20-d-old L-QKO mice. $n = 3$ pairs, $p < 0.0005$ for both plots.

closer to innate γδ T cells than the conventional T cells that perform adaptive immune functions. Our study raised the possibility that E protein–mediated regulation may function upstream of PLZF and other innate lineage-relevant transcription factors. The genetic models established in this study identified E proteins as an important transcriptional switch controlling lineage choice between iNKT and other alternative T cell lineages.

Acknowledgments

We thank Drs. A. Lasorella and A. Iavarone for sharing the *Id2*^{f} strain; Dr. D. Sant'Angelo for providing the PLZF Ab; Dr. M. Krangel for insightful discussion throughout the course of the experiments; Dr. S. Unniraman for advice on DNA methylation assays; Dr. Sophia Sarafova for critiques; B. Zhang, Y. Lin, and I. Belle (Zhuang Laboratory) for comments and critiques; M. Dai for technical assistance in generating the initial L-DKO breeding colony; the Duke Cancer Center Flow Cytometry Facility for assistance in cell sorting; the Duke Cancer Center Sequencing Facility for assistance in Ion Torrent sequencing analysis; and the National Institutes of Health Tetramer Facility for providing CD1d tetramer.

Disclosures

The authors have no financial conflicts of interest.

References

1. Bendelac, A., P. B. Savage, and L. Teyton. 2007. The biology of NKT cells. *Annu. Rev. Immunol.* 25: 297–336.
2. Kawano, T., J. Cui, Y. Koezuka, I. Toura, Y. Kaneko, K. Motoki, H. Ueno, R. Nakagawa, H. Sato, E. Kondo, et al. 1997. CD1d-restricted and TCR-mediated activation of vα14 NKT cells by glycosylceramides. *Science* 278: 1626–1629.
3. Brennan, P. J., M. Brigl, and M. B. Brenner. 2013. Invariant natural killer T cells: an innate activation scheme linked to diverse effector functions. *Nat. Rev. Immunol.* 13: 101–117.
4. Koseki, H., K. Imai, F. Nakayama, T. Sado, K. Moriwaki, and M. Taniguchi. 1990. Homogenous junctional sequence of the V14^{+} T-cell antigen receptor alpha chain expanded in unprimed mice. *Proc. Natl. Acad. Sci. USA* 87: 5248–5252.
5. Girardi, E., I. Maricic, J. Wang, T. T. Mac, P. Iyer, V. Kumar, and D. M. Zajonc. 2012. Type II natural killer T cells use features of both innate-like and conventional T cells to recognize sulfatide self antigens. *Nat. Immunol.* 13: 851–856.
6. Patel, O., D. G. Pellicci, S. Gras, M. L. Sandoval-Romero, A. P. Uldrich, T. Mallevaey, A. J. Clarke, J. Le Nours, A. Theodossis, S. L. Cardell, et al. 2012. Recognition of CD1d-sulfatide mediated by a type II natural killer T cell antigen receptor. *Nat. Immunol.* 13: 857–863.
7. Park, S. H., A. Weiss, K. Benlagha, T. Kyin, L. Teyton, and A. Bendelac. 2001. The mouse CD1d-restricted repertoire is dominated by a few autoreactive T cell receptor families. *J. Exp. Med.* 193: 893–904.
8. Arrenberg, P., R. Halder, Y. Dai, I. Maricic, and V. Kumar. 2010. Oligoclonality and innate-like features in the TCR repertoire of type II NKT cells reactive to a β-linked self-glycolipid. *Proc. Natl. Acad. Sci. USA* 107: 10984–10989.
9. Gapin, L., J. L. Matsuda, C. D. Surh, and M. Kronenberg. 2001. NKT cells derive from double-positive thymocytes that are positively selected by CD1d. *Nat. Immunol.* 2: 971–978.
10. Bezbradica, J. S., T. Hill, A. K. Stanic, L. Van Kaer, and S. Joyce. 2005. Commitment toward the natural T (iNKT) cell lineage occurs at the CD4^{+}8^{+} stage of thymic ontogeny. *Proc. Natl. Acad. Sci. USA* 102: 5114–5119.
11. Egawa, T., G. Eberl, I. Taniuchi, K. Benlagha, F. Geissmann, L. Hennighausen, A. Bendelac, and D. R. Littman. 2005. Genetic evidence supporting selection of the Vα14i NKT cell lineage from double-positive thymocyte precursors. *Immunity* 22: 705–716.
12. Makino, Y., R. Kanno, H. Koseki, and M. Taniguchi. 1996. Development of Vα4^{+} NK T cells in the early stages of embryogenesis. *Proc. Natl. Acad. Sci. USA* 93: 6516–6520.
13. MacDonald, H. R. 2002. Development and selection of NKT cells. *Curr. Opin. Immunol.* 14: 250–254.
14. Bain, G., C. B. Cravatt, C. Loomans, J. Alberola-Ila, S. M. Hedrick, and C. Murre. 2001. Regulation of the helix-loop-helix proteins, E2A and Id3, by the Ras-ERK MAPK cascade. *Nat. Immunol.* 2: 165–171.
15. Lee, S. Y., J. Stadanlick, D. J. Kappes, and D. L. Wiest. 2010. Towards a molecular understanding of the differential signals regulating αβ/γδ T lineage choice. *Semin. Immunol.* 22: 237–246.
16. Murre, C., P. S. McCaw, H. Vaessin, M. Caudy, L. Y. Jan, Y. N. Jan, C. V. Cabrera, J. N. Buskin, S. D. Hauschka, A. B. Lassar, et al. 1989. Interactions between heterologous helix-loop-helix proteins generate complexes that bind specifically to a common DNA sequence. *Cell* 58: 537–544.
17. Benezra, R., R. L. Davis, D. Lockshon, D. L. Turner, and H. Weintraub. 1990. The protein Id: a negative regulator of helix-loop-helix DNA binding proteins. *Cell* 61: 49–59.
18. Jones, M. E., and Y. Zhuang. 2011. Stage-specific functions of E-proteins at the β-selection and T-cell receptor checkpoints during thymocyte development. *Immunol. Res.* 49: 202–215.
19. Wojciechowski, J., A. Lai, M. Kondo, and Y. Zhuang. 2007. E2A and HEB are required to block thymocyte proliferation prior to pre-TCR expression. *J. Immunol.* 178: 5717–5726.
20. Jones, M. E., and Y. Zhuang. 2007. Acquisition of a functional T cell receptor during T lymphocyte development is enforced by HEB and E2A transcription factors. *Immunity* 27: 860–870.
21. D'Cruz, L. M., J. Knell, J. K. Fujimoto, and A. W. Goldrath. 2010. An essential role for the transcription factor HEB in thymocyte survival, *Tcra* rearrangement and the development of natural killer T cells. *Nat. Immunol.* 11: 240–249.
22. Jones-Mason, M. E., X. Zhao, D. Kappes, A. Lasorella, A. Iavarone, and Y. Zhuang. 2012. E protein transcription factors are required for the development of CD4^{+} lineage T cells. *Immunity* 36: 348–361.
23. Ueda-Hayakawa, I., J. Mahlios, and Y. Zhuang. 2009. Id3 restricts the developmental potential of γδ lineage during thymopoiesis. *J. Immunol.* 182: 5306–5316.
24. Verykokakis, M., M. D. Boos, A. Bendelac, E. J. Adams, P. Pereira, and B. L. Kee. 2010. Inhibitor of DNA binding 3 limits development of murine slam-associated adaptor protein-dependent "innate" γδ T cells. *PLoS ONE* 5: e9303.
25. Rivera, R. R., C. P. Johns, J. Quan, R. S. Johnson, and C. Murre. 2000. Thymocyte selection is regulated by the helix-loop-helix inhibitor protein, Id3. *Immunity* 12: 17–26.
26. Pan, L., J. Hanrahan, J. Li, L. P. Hale, and Y. Zhuang. 2002. An analysis of T cell intrinsic roles of E2A by conditional gene disruption in the thymus. *J. Immunol.* 168: 3923–3932.
27. Guo, Z., H. Li, M. Han, T. Xu, X. Wu, and Y. Zhuang. 2011. Modeling Sjögren's syndrome with Id3 conditional knockout mice. *Immunol. Lett.* 135: 34–42.
28. Niola, F., X. Zhao, D. Singh, A. Castano, R. Sullivan, M. Lauria, H. S. Nam, Y. Zhuang, R. Benezra, D. Di Bernardo, et al. 2012. Id proteins synchronize stemness and anchorage to the niche of neural stem cells. *Nat. Cell Biol.* 14: 477–487.
29. Hager, E., A. Hawwari, J. L. Matsuda, M. S. Krangel, and L. Gapin. 2007. Multiple constraints at the level of TCRα rearrangement impact Vα14i NKT cell development. *J. Immunol.* 179: 2228–2234.
30. Brochet, X., M. P. Lefranc, and V. Giudicelli. 2008. IMGT/V-QUEST: the highly customized and integrated system for IG and TR standardized V-J and V-D-J sequence analysis. *Nucleic Acids Res.* 36(Web Server issue): W503-8.
31. Blankenberg, D., A. Gordon, G. Von Kuster, N. Coraor, J. Taylor, and A. Nekrutenko; Galaxy Team. 2010. Manipulation of FASTQ data with Galaxy. *Bioinformatics* 26: 1783–1785.
32. Alamyar, E., V. Giudicelli, S. Li, P. Duroux, and M. P. Lefranc. 2012. IMGT/HighV-QUEST: the IMGT web portal for immunoglobulin (IG) or antibody and T cell receptor (TR) analysis from NGS high throughput and deep sequencing. *Immunome Res.* 8: 26.
33. Taghon, T., M. A. Yui, R. Pant, R. A. Diamond, and E. V. Rothenberg. 2006. Developmental and molecular characterization of emerging β- and γδ-selected pre-T cells in the adult mouse thymus. *Immunity* 24: 53–64.
34. Schmitt, T. M., and J. C. Zúñiga-Pflücker. 2002. Induction of T cell development from hematopoietic progenitor cells by Delta-like-1 in vitro. *Immunity* 17: 749–756.
35. Alonzo, E. S., and D. B. Sant'Angelo. 2011. Development of PLZF-expressing innate T cells. *Curr. Opin. Immunol.* 23: 220–227.
36. Godfrey, D. I., and S. P. Berzins. 2007. Control points in NKT-cell development. *Nat. Rev. Immunol.* 7: 505–518.
37. Das, R., D. B. Sant'Angelo, and K. E. Nichols. 2010. Transcriptional control of invariant NKT cell development. *Immunol. Rev.* 238: 195–215.
38. Benlagha, K., T. Kyin, A. Beavis, L. Teyton, and A. Bendelac. 2002. A thymic precursor to the NK T cell lineage. *Science* 296: 553–555.
39. Mallevaey, T., J. P. Scott-Browne, J. L. Matsuda, M. H. Young, D. G. Pellicci, O. Patel, M. Thakur, L. Kjer-Nielsen, S. K. Richardson, V. Cerundolo, et al. 2009. T cell receptor CDR2β and CDR3β loops collaborate functionally to shape the iNKT cell repertoire. *Immunity* 31: 60–71.
40. Guo, J., A. Hawwari, H. Li, Z. Sun, S. K. Mahanta, D. R. Littman, M. S. Krangel, and Y. W. He. 2002. Regulation of the TCRα repertoire by the survival window of CD4^{+}CD8^{+} thymocytes. *Nat. Immunol.* 3: 469–476.
41. Lasorella, A., and A. Iavarone. 2006. The protein ENH is a cytoplasmic sequestration factor for Id2 in normal and tumor cells from the nervous system. *Proc. Natl. Acad. Sci. USA* 103: 4976–4981.
42. Seiler, M. P., R. Mathew, M. K. Liszewski, C. J. Spooner, K. Barr, F. Meng, H. Singh, and A. Bendelac. 2012. Elevated and sustained expression of the transcription factors Egr1 and Egr2 controls NKT lineage differentiation in response to TCR signaling. *Nat. Immunol.* 13: 264–271.
43. Lee, Y. J., S. C. Jameson, and K. A. Hogquist. 2011. Alternative memory in the CD8 T cell lineage. *Trends Immunol.* 32: 50–56.
44. Miyazaki, M., R. R. Rivera, K. Miyazaki, Y. C. Lin, Y. Agata, and C. Murre. 2011. The opposing roles of the transcription factor E2A and its antagonist Id3 that orchestrate and enforce the naive fate of T cells. *Nat. Immunol.* 12: 992–1001.
45. Alonzo, E. S., R. A. Gottschalk, J. Das, T. Egawa, R. M. Hobbs, P. P. Pandolfi, P. Pereira, K. E. Nichols, G. A. Koretzky, M. S. Jordan, and D. B. Sant'Angelo. 2010.

Development of promyelocytic zinc finger and ThPOK-expressing innate γδ T cells is controlled by strength of TCR signaling and Id3. *J. Immunol.* 184: 1268–1279.

46. Kreslavsky, T., A. K. Savage, R. Hobbs, F. Gounari, R. Bronson, P. Pereira, P. P. Pandolfi, A. Bendelac, and H. von Boehmer. 2009. TCR-inducible PLZF transcription factor required for innate phenotype of a subset of γδ T cells with restricted TCR diversity. *Proc. Natl. Acad. Sci. USA* 106: 12453–12458.
47. Bezman, N. A., C. C. Kim, J. C. Sun, G. Min-Oo, D. W. Hendricks, Y. Kamimura, J. A. Best, A. W. Goldrath, and L. L. Lanier; Immunological Genome Project Consortium. 2012. Molecular definition of the identity and activation of natural killer cells. *Nat. Immunol.* 13: 1000–1009.